



## Fabrication of blend biodegradable nanofibrous nonwoven mats via multi-jet electrospinning

Bin Ding<sup>a,b</sup>, Eiji Kimura<sup>a</sup>, Tomokazu Sato<sup>a</sup>, Shiro Fujita<sup>a</sup>, Seimei Shiratori<sup>a,b,\*</sup>

<sup>a</sup>Graduate School of Science and Technology, Keio University, Yokohama 223-8522, Japan

<sup>b</sup>Shiratori Nanotechnology Company Limited, Kawasaki 212-0054, Japan

Received 25 October 2003; received in revised form 5 January 2004; accepted 17 January 2004

### Abstract

A series of blend biodegradable nanofibrous mats comprising poly(vinyl alcohol) (PVA) and cellulose acetate (CA) were prepared via multi-jet electrospinning. A relative high voltage (20 kV) was used to supply the power for multi-jet electrospinning. The weight ratio of PVA/CA in blend nanofibrous mats can be controlled by changing the number ratio of jets of PVA/CA. Moreover, the real composition of PVA and CA in blend nanofibrous mats was determined by immersing the blend nanofibrous mats into water to remove the PVA component. Morphology, dispersibility, and mechanical properties of blend nanofibrous mats were examined by field emission scanning electron microscopy (FE-SEM), Fourier transform infrared (FT-IR) spectroscopy, wide-angle X-ray diffraction (WAXD), and tensile test. The results showed that the blend nanofibrous mats have good dispersibility. Additionally, the mechanical properties of blend nanofibrous mats were largely influenced by the weight ratio of PVA/CA in blends. Potential applications of the blend nanofibrous mats include filters and biomedical materials.

© 2004 Elsevier Ltd. All rights reserved.

**Keywords:** Multi-jet electrospinning; Blend nanofibrous mats; Dispersibility

### 1. Introduction

In past decades, electrospinning technique has attracted great attention because polymer nanofibers with high surface-to-volume ratio can be fabricated by using this technique [1–5]. Polymer nanofibers have a broad range of applications such as tissue engineering [6], sensor [7], protective clothing [8], filter [9], etc. A number of processing techniques are combined with electrospinning to get functional nanofibrous mats such as electrospinning the mixture of polymer with sol–gel solution [10,11], the mixture of blends of polymers in the same solvent [12,13], the mixture of single polymer in co-solvent [14], and the mixture of polymer solution with nanomaterials [15–17]. Additionally, a novel method was reported by Sun et al. to fabricate the compound core/shell polymer nanofibers by co-electrospinning [18].

Recently, Gupta et al. [19] prepared blend nanofibers of bicomponent system by using a side-by-side electrospinning fashion under fixed state. We sought to increase the dispersibility of multi-component in the blend nanofibrous mats in order to get uniform properties of blend nanofibrous mats. Hence, we designed a multi-jet electrospinning device to afford the opportunity for electrospinning not only bicomponent but also multi-component. Meanwhile, the movable multi-jet and rotatable grounded tubular layer is adopted to get the uniform thickness of blend nanofibrous mats with good dispersibility of multi-component. This approach can be used to fabricate blend nanofibrous mats with multi-component polymers which cannot be dissolved in the same solvent or kept in the same container (polyanion and polycation).

Poly(vinyl alcohol) (PVA), a water-soluble polyhydroxy polymer, has excellent chemical resistance, physical properties, and complete biodegradability which led to broad practical applications. PVA nanofibrous mats are already prepared by electrospinning the aqueous PVA solution and crosslinked with chemical crosslinking agent [20]. Cellulose acetate (CA) is a particularly useful polymer to prepare

\* Corresponding author. Address: Graduate School of Science and Technology, Keio University, Yokohama 223-8522, Japan. Tel.: +81-455-661-602; fax: +81-455-661-587.

E-mail addresses: [shiratori@appi.keio.ac.jp](mailto:shiratori@appi.keio.ac.jp) (S. Shiratori), [binding@appi.keio.ac.jp](mailto:binding@appi.keio.ac.jp) (B. Ding).

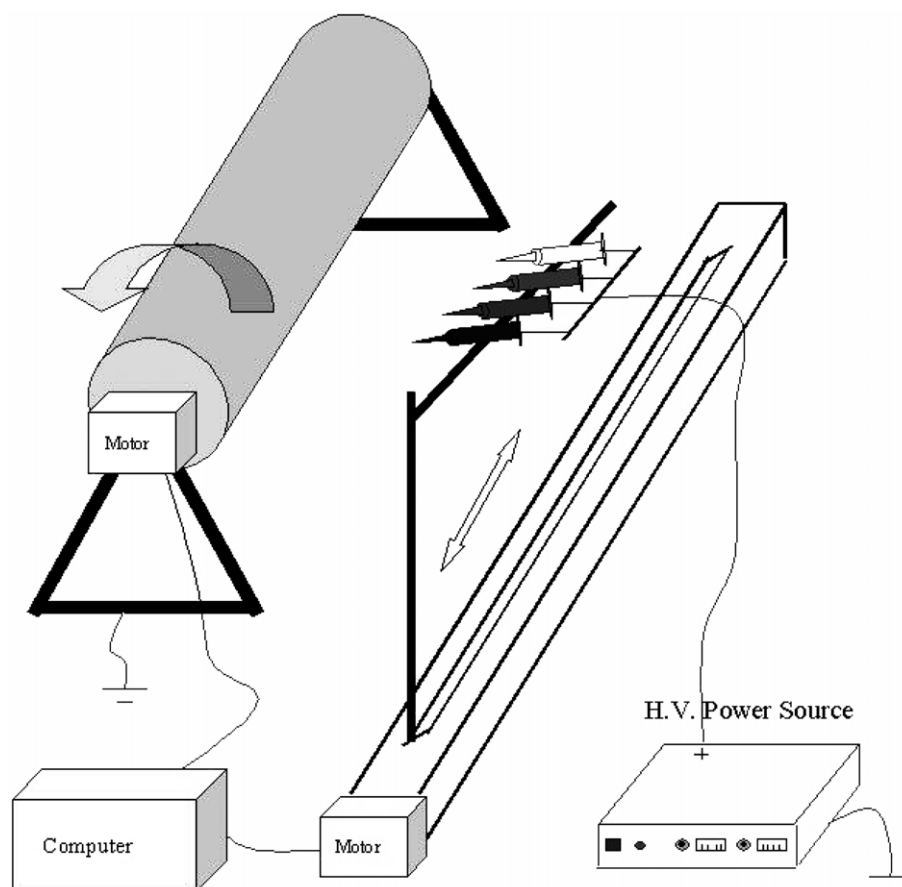


Fig. 1. Schematic of the electrospinning process.

hybrid materials because it can be easily molded into different forms such as membranes, fibers and spheres. The performance of CA may be improved by blending it with appropriate polymers in view of the fact that polymer blends have provided an efficient way to fulfil new requirements for material properties [21]. Preparation and morphology study of CA nanofibrous mats are reported by Liu and Hsieh [14]. Additionally, PVA and CA are both biodegradable polymers, which have no pollution to environment. Therefore, the new nanofibrous materials based on PVA and CA are expected to have both advantages of PVA and CA.

However, the blend nanofibrous mats of PVA and CA have not been reported because it is difficult to find a good solvent for preparing the blend solution of PVA and CA. In the current work, we try to fabricate a series of blend nanofibrous nonwoven mats of PVA and CA with multi-jet electrospinning method and study their morphology, dispersibility, and mechanical properties.

## 2. Experimental

### 2.1. Preparation and properties of polymer solution

A 10 wt% PVA ( $M_n$  66,000) (Wako Pure Chemical

Industries, Ltd., Japan) solution was prepared from PVA powder and distilled water at 80 °C with vigorous stirring. CA ( $M_n$  40,000) (Teijin Co. Ltd., Japan) solution was produced in acetone and *N,N*-dimethylacetamide (DMAc), the weight ratio of acetone to DMAc was 2:1. The concentration of CA solution tested was 10 wt%.

The viscosity and conductivity of PVA and CA solutions were measured by a viscotester (6L/R, Hakke, USA) and electric conductivity meter (CM-40G, TOA DKK Co., Japan), respectively.

### 2.2. Generation of blend nanofibrous mats

The schematic of the electrospinning process was shown in Fig. 1. A grounded stainless tubular layer was covered by a piece of aluminum foil and rotated [22] at 100 rpm. A multi-jet containing four plastic syringes (5 ml) were clamped to a stand which can be moved with the speed of 20 m/min along the track. The distance between two tips was 3 cm. The velocity of the rotatable tubular layer and the movable stand can be controlled by computer. The PVA and CA solutions were placed in different syringes according to the requirement. The positive electrode of a high voltage power supply (FC30P4, Glassman High Voltage Inc., USA) was connected with copper wires, which immersed in

Table 1  
Properties of PVA and CA solutions

Sample	Concentration (wt%)	Viscosity (centipoises)	Conductivity (ms/m)	Throughput (mg/min jet)
PVA solution	10	420	18.6	1.9
CA solution	10	360	0.3	2.3

polymer solutions. The voltage was 20 kV, and tip-to-collector distance (TCD) was 15 cm. The number ratio of jets of PVA/CA was controlled with 4/0, 3/1, 2/2 and 0/4 to get blend nanofibrous mats with different weight ratio of PVA/CA. The homogenous nanofibrous nonwoven mats were collected on the surface of aluminum foil and dried at 80 °C in vacuum for 24 h.

### 2.3. Determination of composition of PVA and CA in blend nanofibrous mats

The composition of PVA and CA in blend nanofibrous mats was investigated by immersing the dried blend nanofibrous mats into distilled water to remove the PVA component. The immersion time was 48 h. Then, the wet nanofibrous mats were dried at 80 °C in vacuum for 24 h. The content of PVA was calculated with the weight loss during immersion. Each sample for immersion test was checked 10 times.

### 2.4. Characterization techniques

The morphology and diameter of nanofibrous mats were determined with field emission scanning electron microscopy (FE-SEM) (S-4700, Hitachi Ltd., Japan). The diameters of nanofibers were measured by using image analyzer (Adobe Photoshop 7.0). FT-IR spectra were recorded using a BIO-RAD FTS-60A/896 FT-IR spectrometer in the range 4000–400  $\text{cm}^{-1}$ . The measurement of the crystallinity was carried out at room temperature with a wide-angle X-ray diffractometer (RTP300, Rigaku Co., Japan). The diffraction scans were collected at  $2\theta = 5 - 40^\circ$  with the speed of  $1^\circ/\text{min}$ .

The mechanical properties of nanofibrous mats were tested on a tensile tester (AGS-100A, Shimadzu Co., Japan) with the extension rate of 10 mm/min. The size of the samples was 100 mm length, 20 mm width, 50 mm distance between two clamps.

Table 2  
Compositions of nanofibrous mats

Sample	No. ratio of jets (PVA/CA)	Arithmetical weight ratio (PVA/CA)	Real weight ratio (PVA/CA)	Average fiber diameter (nm)
A	4/0	100/0	100/0	190
B	3/1	70/30	77/23	220
C	2/2	45/55	51/49	240
D	1/3	20/80	26/74	290
E	0/4	0/100	0/100	420

## 3. Results and discussion

### 3.1. Electrospinning process and determination of composition in blends

Table 1 lists solution properties of PVA and CA. The nanofibrous mats can be fabricated under the given viscosity and conductivity from each polymer solutions. During electrospinning process, a relative high voltage (20 kV) was used to supply the power for four jets electrospinning. The PVA and CA nanofibers were alternatively and continuously deposited on the collector because of the movable multi-jet and the rotatable collector. The throughput of PVA and CA nanofibers was 1.9 and 2.3 mg/min jet when all four jets were placed with the same solution during electrospinning, respectively.

The relation between weight ratio of PVA/CA and number ratio of jets of PVA/CA is given in Table 2. The weight ratio of PVA/CA in calculation was deduced from the throughput of each polymer with corresponding amount of jets. Moreover, the real weight ratio of PVA/CA was investigated through the immersion test. Water was a suitable medium for the immersion test because PVA was soluble in water. From the results of the real weight ratio of PVA/CA, it can be observed that the PVA component in blend nanofibrous mats can be dissolved entirely to leave CA in fiber state. And there was no weight loss for CA nanofibrous mats during the immersion test.

However, some differences were found between the calculation and fact in weight ratio of PVA/CA. One reason maybe was due to that the throughput of PVA and CA was measured when all four jets were placed with the same kind of solution. The distribution of current for different jets was changed when four jets were contained with different kinds of polymer solutions because of their different viscosity and conductivity. A linear relation was found between the currents and flow rates by Shin et al. [3]. The PVA solution has much higher conductivity (18.6 ms/m) than CA solution (0.3 ms/m). Another reason maybe was due to the throughput in electrospinning could not be kept constant for the competition between the mechanical and electric

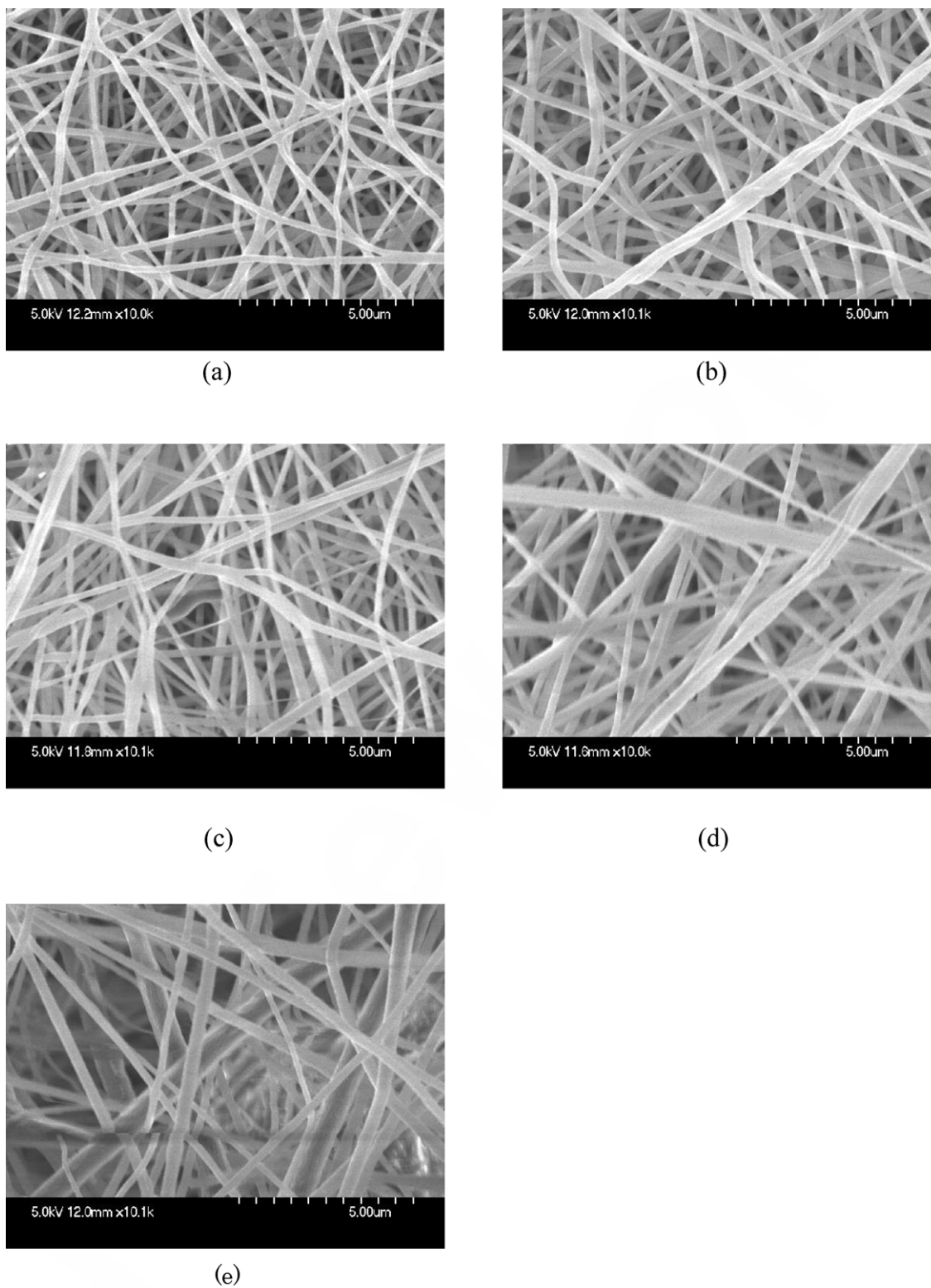


Fig. 2. FE-SEM photographs of nanofibrous mats with different number ratio of jets of PVA/CA. (a) 4/0; (b) 3/1; (c) 2/2; (d) 1/3; (e) 0/4.

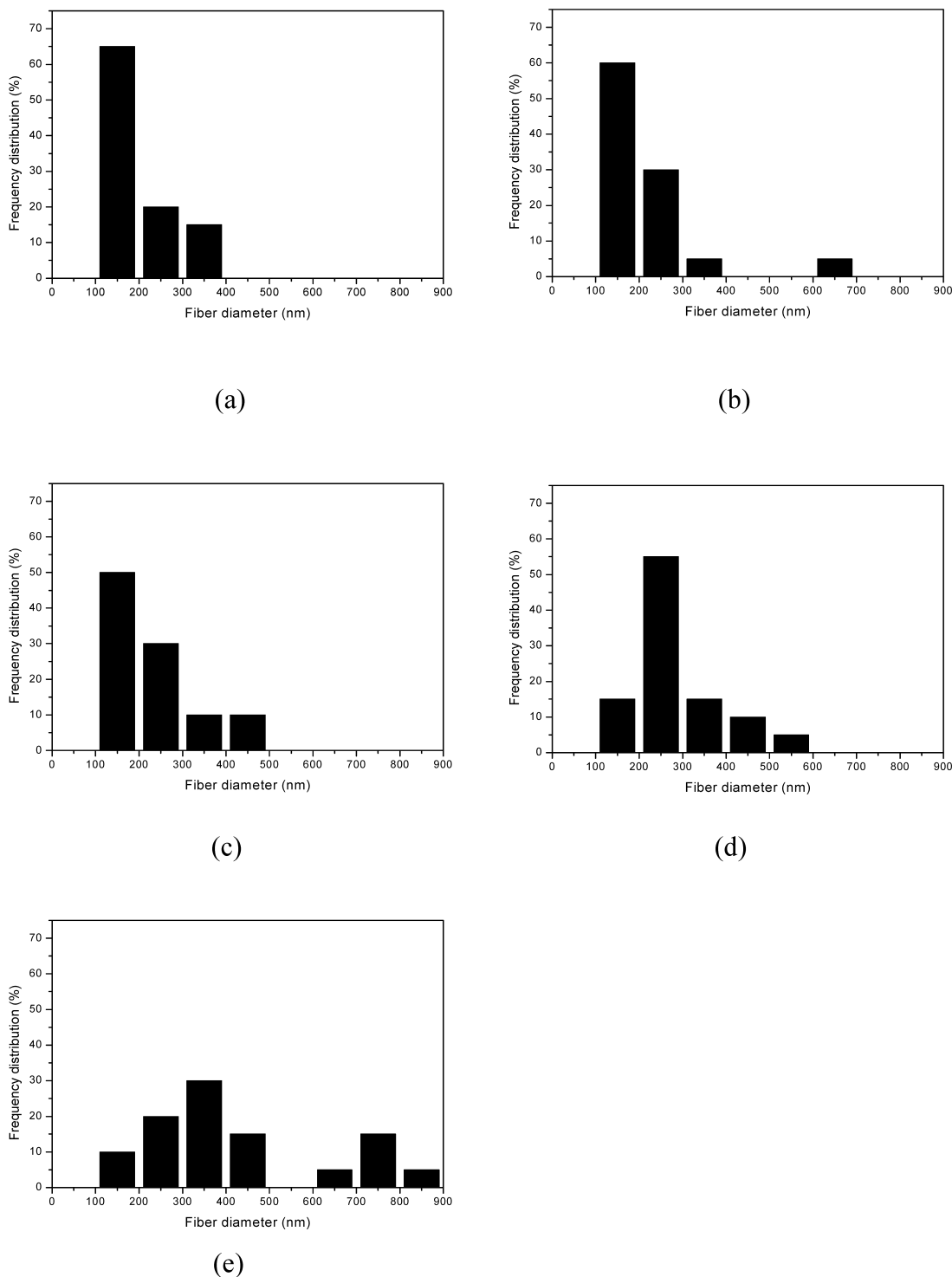


Fig. 3. Nanofiber diameter distributions of nanofibrous mats with different number ratio of jets of PVA/CA. (a) 4/0; (b) 3/1; (c) 2/2; (d) 1/3; (e) 0/4.

forces. Hence, the real content of PVA in blend nanofibrous mats was different with the arithmetical content which only deduced from the throughput.

### 3.2. Morphology of nanofibrous mats

Fig. 2 shows FE-SEM photographs of PVA, CA, and

blend nanofibers. The morphology of the pure PVA nanofibers (Fig. 2(a)) was regular and had an average diameter of 190 nm. In Fig. 2(e), it was observed that the diameters of pure CA nanofibers were broadly distributed with an average diameter of 420 nm. A similar phenomenon of CA nanofibers morphology was reported by Liu and Hsieh [14]. Fig. 2(b)–(d) provide the morphology of blend

nanofibers of PVA and CA. The diameters of blend nanofibers became irregular because of the existence of CA nanofibers. Meanwhile, the average diameters of blend nanofibers were increased from 220 to 290 nm on decreasing the number ratio of jets of PVA/CA from 3/1 to 1/3 (Table 2).

The diameter distributions of nanofibrous mats with different number ratio of jets of PVA/CA are presented in Fig. 3. The region of distribution of pure PVA nanofibers (Fig. 3(a)) was ranged from 100 to 400 nm and the majority was in the range of 100 to 200 nm. However, the diameters of pure CA nanofibers (Fig. 3(e)) were broadly distributed in the range of 100–900 nm with two major regions. The regions of diameter distributions of blend nanofibrous mats were enlarged and the major region was moved to large diameter when the number ratio of jets of PVA/CA was decreased from 3/1 to 1/3 (Fig. 3(b)–(d)). It can be deduced that the percentage of CA component was increased with decreasing the number ratio of jets of PVA/CA.

### 3.3. Fourier transform infrared spectroscopy

Fig. 4 gives the FT-IR spectra of nanofibrous mats with different number ratio of jets of PVA/CA. Both PVA nanofibers (curve a in Fig. 4) and CA nanofibers (curve e in Fig. 4) exhibited a number of FT-IR absorption features below  $2000\text{ cm}^{-1}$ . These major absorption features appeared at  $1740\text{ cm}^{-1}$  (C=O),  $1450\text{ cm}^{-1}$  (O=C-OR),  $1340\text{ cm}^{-1}$  ( $-\text{CH}_2$ ), and  $1110\text{ cm}^{-1}$  (C-O-C) [23,24]. Features above  $2000\text{ cm}^{-1}$  are both intense and composition sensitive. They appeared at  $2900\text{ cm}^{-1}$  ( $-\text{CH}_2$ ) and  $3400\text{ cm}^{-1}$  ( $-\text{OH}$ ).

Additionally, PVA nanofiber has a typical band around  $860\text{ cm}^{-1}$  and CA nanofiber has typical bands around  $1190$  and  $1150\text{ cm}^{-1}$  [23,24]. These peaks around  $3400$ ,  $2900$  and  $1450\text{ cm}^{-1}$  became weaker, two shoulder peaks around  $1110\text{ cm}^{-1}$  and the peak around  $860\text{ cm}^{-1}$  were disappeared on decreasing the number ratio of jets of PVA/CA from 4/0 to 0/4. Meanwhile, the peaks around  $1190$  and  $1150\text{ cm}^{-1}$

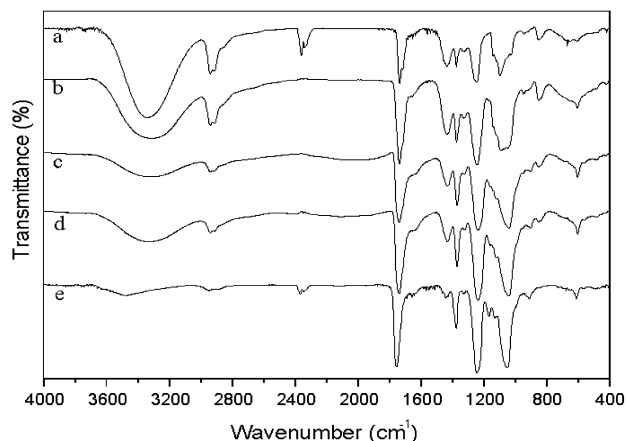


Fig. 4. FT-IR spectra of nanofibrous mats with different number ratio of jets of PVA/CA. (a) 4/0; (b) 3/1; (c) 2/2; (d) 1/3; (e) 0/4.

were more evident with decreasing the number ratio of jets of PVA/CA from 4/0 to 0/4. It was also observed that all the blend nanofibers (curves b to d in Fig. 4) have both IR features of PVA and CA without new peaks. The results demonstrated that there was no chemical reaction between PVA and CA nanofibers, just physical blending. Moreover, the intensities of feature peaks of PVA and CA in blend nanofibrous mats were strongly affected by the weight ratio of PVA/CA. The feature peaks of nanofibrous mats were gradually transformed from PVA to CA with decreasing the number ratio of PVA/CA from 4/0 to 0/4. The regular transforms indicated that PVA and CA nanofibers dispersed into each other very well.

### 3.4. Wide-angle X-ray diffraction

The WAXD patterns of nanofibrous mats with different number ratio of jets of PVA/CA are shown in Fig. 5. As observed in the curve a of Fig. 5, one peak around  $2\theta = 20^\circ$  appeared, corresponding to the (101) plane of PVA semicrystalline in pure PVA nanofibers [11]. Pure CA nanofibers (curve e in Fig. 5) also showed a weak amorphous peak [25]. It indicated the amorphous nature of PVA and CA nanofibers. The intensity of amorphous peaks ( $2\theta = 20^\circ$ ) of nanofibrous mats gradually decreased with decreasing the number ratio of jets of PVA/CA. The characteristics of WAXD patterns of nanofibrous mats were gradually transformed from PVA to CA with decreasing the number ratio of PVA/CA from 4/0 to 0/4. It also proved that the weight ratio of PVA/CA in blend nanofibrous mats can be controlled by changing the number ratio of jets of PVA/CA.

### 3.5. Mechanical properties

The mechanical properties of electrospun blend nanofibrous mats were strongly influenced by the properties of

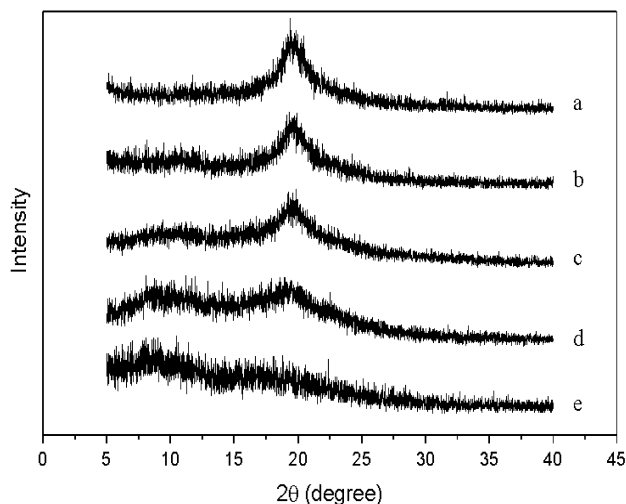


Fig. 5. WAXD patterns of nanofibrous mats with different number ratio of jets of PVA/CA. (a) 4/0; (b) 3/1; (c) 2/2; (d) 1/3; (e) 0/4.

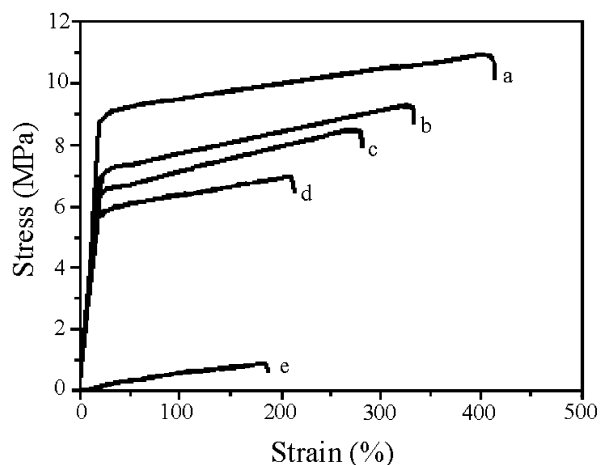


Fig. 6. Stress–strain behavior of nanofibrous mats with different number ratio of jets of PVA/CA. (a) 4/0; (b) 3/1; (c) 2/2; (d) 1/3; (e) 0/4.

each polymer in the blend nanofibrous mats, nanofiber structure, and the interaction between each polymer nanofibers [26]. Stress–strain behavior of nanofibrous mats with different number ratio of jets of PVA/CA is shown in Fig. 6. The nanofibrous mats were broken when the maximum amount of tensile stress (tensile strength) applied to them. After adding with PVA component, the mechanical properties of CA nanofibrous mats were largely reinforced. The resulting modulus, tensile strength, and yield stress of nanofibrous mats are shown in Fig. 7. CA nanofibrous mats (0/4) showed much weaker mechanical properties compared with PVA nanofibrous mats (4/0). The modulus of blend nanofibrous mats were increased from 18.1 to 34.0 MPa with increasing the number ratio of jets of PVA/CA from 1/3 to 3/1. Meanwhile, the tensile strength and yield stress also were increased from 7.0 to 9.4 MPa and from 5.9 to 7.2 MPa on increasing the number ratio of jets of PVA/CA from 1/3 to 3/1, respectively.

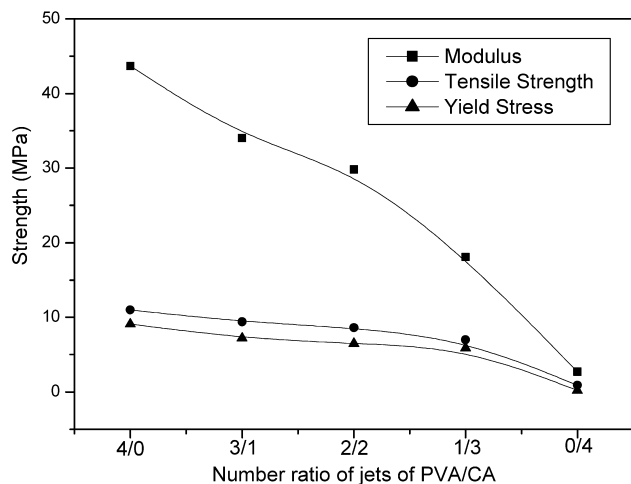


Fig. 7. Modulus, tensile strength and yield stress of nanofibrous mats as a function of number ratio of jets of PVA/CA.

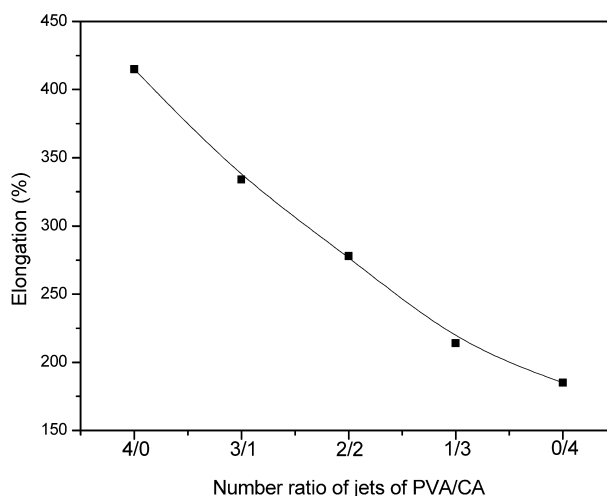


Fig. 8. Elongation of nanofibrous mats as a function of number ratio of jets of PVA/CA.

Fig. 8 presents the elongation of nanofibrous mats as a function of number ratio of jets of PVA/CA. As observed, the elasticity of blend nanofibrous mats was reinforced with addition of PVA component. The breaking elongation of the blend nanofibrous mats gradually increased from 214 to 334% with increasing the number ratio of jets of PVA/CA from 1/3 to 3/1. As a result, the mechanical properties of blend nanofibrous mats were improved with increasing the content of PVA. Moreover, it also indicated that the blend nanofibrous mats have good dispersibility of PVA and CA nanofibers to lead uniform mechanical properties for each sample.

#### 4. Conclusions

Blend biodegradable nanofibrous nonwoven mats with different weight ratio of PVA/CA were successfully fabricated via multi-jet electrospinning. These nanofibrous mats were examined regarding their morphology, dispersibility, and mechanical properties. The results showed the blend nanofibrous mats have good dispersibility because the blend nanofibrous mats have uniform properties for each sample and regular transforms with changing the number ratio of jets of PVA/CA. As a result, the PVA and CA nanofibers were homogenously dispersed into each other. FT-IR results demonstrated that there was no chemical reaction between PVA and CA nanofibers, just physical blending. Additionally, the mechanical properties of CA nanofibrous mats were improved by increasing the content of PVA nanofibers. Furthermore, the multi-component blend nanofibrous mats also can be obtained by increasing the electrospinning jets in this multi-jet electrospinning fashion.

## Acknowledgements

This work was partly supported by 21 century COE Keio University program (KEIO LCC COE21), Japan.

## References

- [1] Reneker DH, Chun I. *Nanotechnology* 1996;7:216–23.
- [2] Deitzel JM, Kleinmeyer J, Harris D, Beck TNC. *Polymer* 2001;42: 261–72.
- [3] Shin YM, Hohman MM, Brenner MP, Rutledge GC. *Polymer* 2001; 42:9955–67.
- [4] Reneker DH, Yarin AL, Fong H, Koombhongse S. *J Appl Phys* 2000; 87:4531–47.
- [5] Yarin AL, Koombhongse S, Reneker DH. *J Appl Phys* 2001;89: 3018–26.
- [6] Matthews JA, Wnek GE, Simpson DG, Bowlin GL. *Biomacromolecules* 2002;3:232–8.
- [7] Wang XY, Drew C, Lee SH, Senecal KJ, Kumar J, Samuelson LA. *Nanoletters* 2002;2:1273–5.
- [8] Schreuder-Gibson HL, Gibson P, Senecal K, Sennett M, Walker J, Yeomans W, et al. *J Adv Mater* 2002;34:44–55.
- [9] Tsai PP, Schreuder-Gibson H, Gibson P. *J Electrostat* 2002;54: 333–41.
- [10] Ding B, Kim HY, Kim CK, Khil MS, Park SJ. *Nanotechnology* 2003; 14:532–7.
- [11] Shao CL, Kim HY, Gong J, Ding B, Lee DR, Park SJ. *Mater Lett* 2003;57:1579–84.
- [12] Norris ID, Shaker MM, Ko FK, MacDiarmid AG. *Synth Met* 2000; 114:109–14.
- [13] Kenawy ER, Bowlin GL, Mansfield K, Laman J, Simpson DG, Sanders EH, Wnek GE. *J Controlled Release* 2002;81:57–64.
- [14] Liu HQ, Hsieh YL. *J Polym Sci, Polym Phys* 2002;40:2119–29.
- [15] He CH, Gong J. *Polym Degrad Stab* 2003;81:117–24.
- [16] Ko F, Gogotsi Y, Ali A, Naguib N, Ye H, Yang GL, Li C, Willis P. *Adv Mater* 2003;15:1161–5.
- [17] Dror Y, Salalha W, Khalfin RL, Cohen Y, Yarin AL, Zussman E. *Langmuir* 2003;19:7012–20.
- [18] Sun Z, Zussman E, Yarin AL, Wendorff JH, Greiner A. *Adv Mater* 2003;15:1929–32.
- [19] Gupta P, Wilkes GL. *Polymer* 2003;44:6353–9.
- [20] Ding B, Kim HY, Lee SC, Shao CL, Lee DR, Park SJ, Kwag GB, Choi KJ. *J Polym Sci, Polym Phys* 2002;40:1261–8.
- [21] Sajitha CJ, Mohan D. *Polym Int* 2003;52:138–45.
- [22] Theron A, Zussman E, Yarin AL. *Nanotechnology* 2001;12:384–90.
- [23] Ryu JH, Lee HJ, Kim YJ, Kang YS, Kim HS. *Chem Eur J* 2001;7: 1525–9.
- [24] Yu YH, Lin CY, Yeh JM, Lin WH. *Polymer* 2003;44:3553–60.
- [25] Zhou Q, Zhang LN, Zhang M, Wang B, Wang SJ. *Polymer* 2003;44: 1733–9.
- [26] Lee KH, Kim HY, Ryu YJ, Kim KW, Choi SW. *J Polym Sci, Polym Phys* 2003;41:1256–62.